1521-009X/41/1/132–140$25.00
Drug Metabolism and Disposition

http://dx.doi.org/10.1124/dmd.112.048736
Drug Metab Dispos 41:132–140, January 2013

Generation and Characterization of a Novel *Cyp2a(4/5)bgs*-Null Mouse Model

Yuan Wei, Lei Li, Xin Zhou, Qing-Yu Zhang, Anwar Dunbar, Fang Liu, Kerri Kluetzman, Weizhu Yang, and Xinxin Ding

Wadsworth Center, New York State Department of Health, and School of Public Health, State University of New York at Albany, New York

Received August 29, 2012; accepted October 15, 2012

ABSTRACT

Knockout mouse models targeting various cytochrome P450 (P450 or CYP) genes are valuable for determining P450's biologic functions, including roles in drug metabolism and chemical toxicity. In this study, a novel *Cyp2a(4/5)bgs*-null mouse model was generated, in which a 1.2-megabase pair genomic fragment containing nine *Cyp* genes in mouse chromosome 7 (including, sequentially, *Cyp2a5*, *2g1*, *2b19*, *2b23*, *2a4*, *2b9*, *2b13*, *2b10*, and *2s1*) are deleted, through *Cre*-mediated recombination in vivo. The resultant mouse strain was viable and fertile, without any developmental deficits or morphologic abnormalities. Deletion of the constitutive genes in the cluster was confirmed by polymerase chain reaction analysis of the genes and the mRNAs in tissues known to express each gene. The loss of this gene cluster led to significant decreases in microsomal activities toward testosterone hydroxylation in various tissues examined, including olfactory mucosa (OM), lung, liver, and brain. In addition, systemic clearance of pentobarbital was decreased in *Cyp2a(4/5)bgs*-null mice, as indicated by >60% increases in pentobarbital-induced sleeping time, compared with wild-type (WT) mice. This novel *Cyp2a(4/5)bgs*-null mouse model will be valuable for in vivo studies of drug metabolism and chemical toxicities in various tissues, including the liver, lung, brain, intestine, kidney, skin, and OM, where one or more of the targeted *Cyp* genes are known to be expressed in WT mice. The model will also be valuable for preparation of humanized mice that express human CYP2A6, CYP2A13, CYP2B6, or CYP2S1, and as a knockout mouse model for five non-P450 genes (*Vmn1r184*, *Nalp9c*, *Nalp4a*, *Nalp9a*, and *Vmn1r185*) that were also deleted.

Introduction

The human *CYP2* gene cluster located on chromosome 19 consists of all genes/pseudogenes in the *CYP2A*, *2B*, *2F*, *2G*, *2S*, and *2T* subfamilies (Hoffman et al., 2001). The corresponding gene subfamilies (*Cyp2a, 2b, 2f, 2g, 2s,* and *2t*) are also clustered in the mouse genome (Wang et al., 2003), on chromosome 7, which is known to be syntenic to human chromosome 19. These various *Cyp2* genes are preferentially expressed in the respiratory tract, although some *Cyp2a* and *Cyp2b* genes are also expressed in the liver and elsewhere. Many of the cytochrome P450 (P450) enzymes encoded by the *Cyp2* gene cluster are known to be active in the metabolism of numerous substrates, including therapeutic drugs, toxicants, and endogenous compounds (Su and Ding, 2004; Zhang and Ding, 2008).

Cyp knockout mice can be used to study the precise role of P450 enzymes in drug metabolism and chemical-induced toxicity in vivo (Gonzalez, 2003). Among genes of the *Cyp2* cluster, single-gene knockout models have been generated previously for *Cyp2a5*, *Cyp2g1*, and *Cyp2f2*, and used to study the specific roles of these P450 enzymes in the metabolism and toxicity of numerous xenobiotics, including nicotine, naphthalene, coumarin, 4-(methylnitrosamino)-1-(3-pyridyl)-1-butanone, dichlobenil, methimazole, and 3-methylindole (Zhou et al., 2010, 2012a,b; Zhuo et al., 2004; Xie et al., 2010, 2011; Li et al., 2011). However, the single-*Cyp* knockout mouse models are often unsatisfactory due to the multiplicity of *Cyp* genes in many of the mouse *Cyp* subfamilies and to the overlapping substrate specificity of the corresponding P450 enzymes. Alternative strategies that would delete multiple *Cyp* genes (e.g., those of the *Cyp3a* subfamily (van Herwaarden et al., 2007) and *Cyp2d* subfamily (Scheer et al., 2012), knockdown the expression of multiple *Cyp* genes (Damiri et al., 2012), or abolish all microsomal P450 activities through deletion or down-regulation of the *Cpr* gene (e.g., Gu et al., 2003; Wu et al., 2005; Wei et al., 2010) have been reported, and the resultant mouse models have been found to have unique advantages for functional studies (e.g., Gu et al., 2005; Weng et al., 2007; Conroy et al., 2010). In this study, we have generated a novel *Cyp2a(4/5)bgs*-null strain in which nine of the *Cyp* genes in a 1.2-megabase pair (Mb) *Cyp2* cluster in mouse chromosome 7 (including, sequentially, *Cyp2a5*, *2g1*, *2b19*, *2b23*, *2a4*, *2b9*, *2b13*, *2b10*, and *2s1*) are removed by using the *Cre*-loxP technology (Nagy, 2000).

The *Cre*-loxP system can be used to delete both small and large DNA fragments on mouse chromosomes (e.g., Yu and Bradley, 2001). Most chromosome engineering strategies involve two consecutive

This work was supported in part by the National Institutes of Health [Grants ES001337, ES007462, CA092596 (to X.D.), and GM082978 (to Q.Z.)].
Y.W. and L.L. contributed equally to this work.
dx.doi.org/10.1124/dmd.112.048736.

ABBREVIATIONS: B6, C57BL/6; bp, base pair; CPR, cytochrome P450 reductase; ES, embryonic stem; HPLC, high-performance liquid chromatography; kb, kilobase pair; LC-MS, liquid chromatography-mass spectrometry; Mb, megabase pair; NADPH, reduced β-nicotinamide adenine dinucleotide phosphate; OH-T, hydroxytestosterone; OM, nasal olfactory mucosa; P450, cytochrome P450; PCR, polymerase chain reaction; WT, wild type.

targeting steps (to insert the two requisite loxP sites, one at a time, at the two predefined ends of a large chromosome fragment). Cre-mediated deletion of the floxed, large DNA fragment can be achieved via either *in vitro* or in vivo methods. In the in vitro method, Cre is introduced into cultured embryonic stem (ES) cells harboring the floxed allele through transfection with a Cre-expressing plasmid. ES cell clones that have undergone the desired recombination event will be identified and used for production of chimeras. As an example, this strategy was used to produce the *Cyp3a*-null mouse model (van Herwaarden et al., 2007). In the in vivo method, two mouse strains, each containing a single loxP site at one end of the targeted genomic fragment, are produced; progenies with the two loxP sites in the same orientation, one at each end of the targeted genomic fragment in either a *trans* or a *cis* configuration, are obtained, and Cre is introduced via further cross-breeding with a Cre-expressing mouse (Brault et al., 2006). In this study, we have successfully generated a 1.2-Mb *Cyp2a (4/5)bgs*-null mouse model using the in vivo approach. The new mouse was produced through cross-breeding, first between an available *Cyp2a5*-null(-loxP) mouse (Zhou et al., 2010) and a newly generated *Cyp2s1*-null(-loxP) mouse (yielding a *cis*-targeted, floxed *Cyp2a(4/5)bgs* allele) and then between the *Cyp2a(4/5)bgs*-floxed mouse and a *Cre*-transgenic mouse.

Homozygous *Cyp2a(4/5)bgs*-null mice were characterized for viability and fertility; growth rates; and potential compensatory expression of other major P450 enzymes that may be involved in drug metabolism and chemical toxicity. The loss of expression of the targeted genes in the cluster was confirmed by RNA-polymerase chain reaction (PCR) analysis of gene expression in tissues known to express the *Cyp* genes in wild-type (WT) mice, and by functional analysis of microsomal metabolism of testosterone (a model P450 substrate) in vitro and pentobarbital clearance in vivo.

Materials and Methods

Chemicals and Reagents. Testosterone, various hydroxytestosterones (OH-T), 16α-OH-progesterone, and other testosterone metabolite standards were obtained from the same sources as previously described (Ding and Coon 1994). Reduced β-nicotinamide adenine dinucleotide phosphate (NADPH), ascorbic acid, and pentobarbital were from Sigma-Aldrich (St. Louis, MO). All high-performance liquid chromatography (HPLC) grade solvents (acetonitrile, methanol, and water) were from Thermo Fisher Scientific (Pittsburgh, PA).

Generation of the Cyp2s1-Null Mouse. All experiments involving animals were approved by the Institutional Animal Care and Use Committee of the Wadsworth Center, New York State Department of Health (Albany, NY). A C57BL/6J (B6) mouse bacterial artificial chromosome clone containing *Cyp2s1* gene, ID number RP24-191C15, was obtained from the BACPAC Resources Center at Children's Hospital & Research Center Oakland (Oakland, CA). A 1.4-kb Nhe I-Sac I fragment (containing *Cyp2s1* exon 2) and a 7.0-kb Pme I-Msc I fragment (containing *Cyp2s1* exons 4-8) were isolated and subcloned into EmbryoMax vector with hygromycin B resistance (Specialty Media, Phillipsburg, NJ). The targeting vector contained, sequentially, the 1.4-kb 5′ homology region, the hygromycin B resistance gene (*hygro*), a loxP site, and the 7.0-kb 3′ homology region (Fig. 1A).

Electroporation and selection of ES cells, as well as blastocyst injection, were performed in the Transgenic and Knockout Core Facility of the Wadsworth Center. The construct was linearized with Spe I before electroporation into ES cells. Bruce 4 ES cells (B6-derived, Kontgen et al., 1993) were used for electroporation. Following electroporation, cells were cultured on tissue culture plates containing mitomycin C-treated primary embryonic fibroblast feeder layers prepared from a transgenic mouse line that expresses the hygromycin B-resistance gene (*hygro*) (Johnson et al., 1995). After 24 hours, the medium was replaced with selection medium containing 100 μg/ml hygromycin B. Hygromycin B-resistant embryonic stem cell clones were screened using PCR, with primers specific for the targeted allele (Table 1); the forward primer (F1) was located upstream of the 1.4-kb Nhe I-Sac I fragment, and the reverse primer (R1) was within the vector region. Positive homologous recombinant clones were confirmed by Southern blot analysis, with both an external probe (P1; a 1.3-kb fragment, beginning at ~200 bp upstream of *Cyp2s1* exon 1) and an internal probe (P2; a 1.3-kb fragment, beginning at ~50 bp downstream of the *hygro* start codon).

Positive ES cell clones were then injected into the blastocysts from albino B6(Cg)-Tyr$^{c\text{-}2J}$/J (stock 000058; The Jackson Laboratory, Bar Harbor, ME) female mice. The blastocysts were transferred into the uterus of a pseudopregnant B6CBAF1/J mouse to generate offspring. The male chimera pups were identified by their black eyes and coat color. Adult chimeras were bred with WT B6 female mice to obtain germline transmission F1 mice that were heterozygous for the mutant allele. Homozygous *Cyp2s1*-null mice were generated by intercrossing the *Cyp2s1*$^{+/-}$ heterozygotes. Genotypic analysis

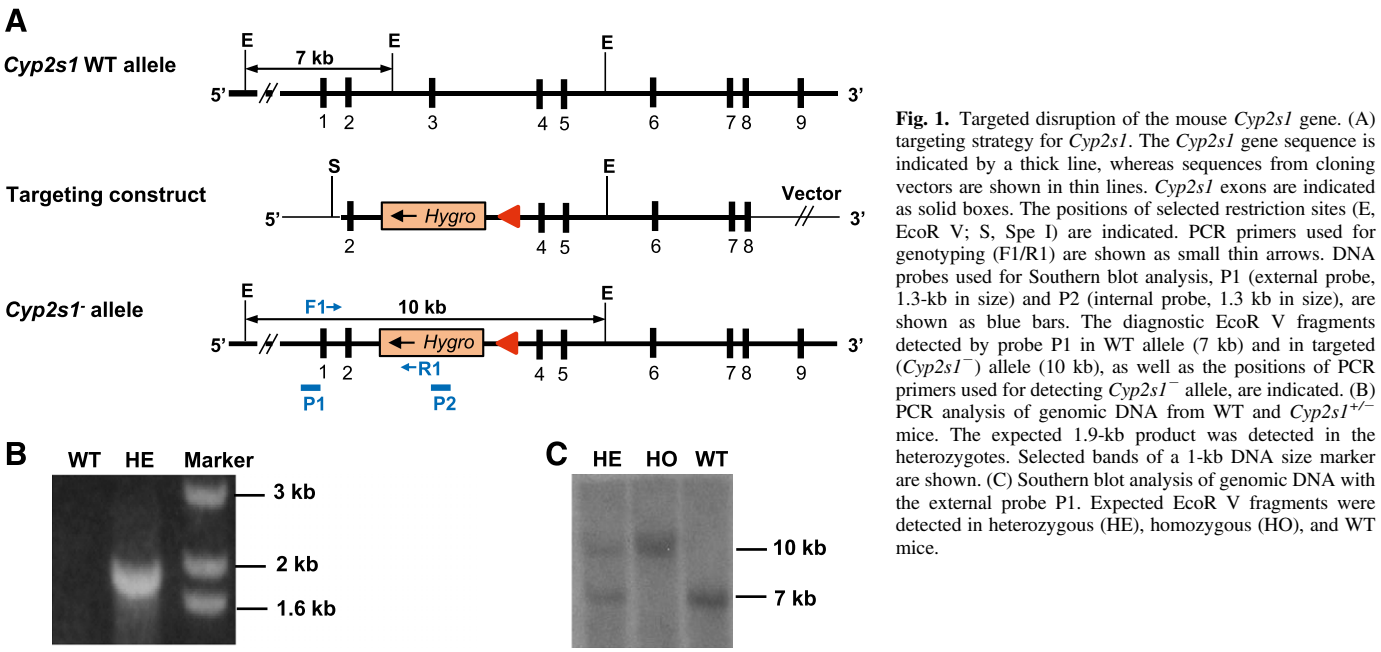

Fig. 1. Targeted disruption of the mouse *Cyp2s1* gene. (A) targeting strategy for *Cyp2s1*. The *Cyp2s1* gene sequence is indicated by a thick line, whereas sequences from cloning vectors are shown in thin lines. *Cyp2s1* exons are indicated as solid boxes. The positions of selected restriction sites (E, EcoR V; S, Spe I) are indicated. PCR primers used for genotyping (F1/R1) are shown as small thin arrows. DNA probes used for Southern blot analysis, P1 (external probe, 1.3-kb in size) and P2 (internal probe, 1.3 kb in size), are shown as blue bars. The diagnostic EcoR V fragments detected by probe P1 in WT allele (7 kb) and in targeted (*Cyp2s1*$^{-}$) allele (10 kb), as well as the positions of PCR primers used for detecting *Cyp2s1*$^{-}$ allele, are indicated. (B) PCR analysis of genomic DNA from WT and *Cyp2s1*$^{+/-}$ mice. The expected 1.9-kb product was detected in the heterozygotes. Selected bands of a 1-kb DNA size marker are shown. (C) Southern blot analysis of genomic DNA with the external probe P1. Expected EcoR V fragments were detected in heterozygous (HE), homozygous (HO), and WT mice.

TABLE 1

Primers used for mouse genotypic analysis

Allele	Forward Primer (5′–3′)	Reverse Primer (5′–3′)	Expected Product Size	Annealing Temperature
				°C
Cyp2s1^{-}	gcgggacttaagtgttcagc	actgtcgggcgtacacaaat	1.9 kb	61
Cyp2a5^{-}	ttagggcactgggtcacttc	cgatctagaggtaccataacttcgt	2.1 kb	62
Cyp2s1–Cyp2a5$^{\Delta}$	cagtctttgagaggcccaag	caagccatgtttttgttgga	493 bp	60
CMV–Cre	ggatttccgtctctggtgtagc	cattgcccctgtttcactatcc	335 bp	65
Cyp2a5	gcgtcctggtcttgatgtct	cccacctggtcagtacccta	224 bp	60
Cyp2g1	tggcactttgtttgtcttgc	tgccatctgtgaccttcatc	196 bp	60
Cyp2a4	gcgtcctggttttgatgtct	cccacctggtcagtacccta	224 bp	60
Cyp2b10	ctctccttgtgggcttcttg	gaacctacaccgtggaagga	243 bp	60
Cyp2s1	cactgaggggaagggaccagtcc	atcagctcctcgccttctcgctt	130 bp	60

was performed for the targeted *Cyp2s1* allele, using the same aforementioned primers for PCR screening of ES cells. Primers for genotyping WT allele are listed in Table 1.

Generation of the Cyp2a(4/5)bgs-Null (Cyp2s1-Cyp2a5$^{\Delta/\Delta}$) Mouse. Generation and characterization of the *Cyp2a5*-null mouse stain harboring a floxed *neo* cassette has been described elsewhere (Zhou et al., 2010). The loxP sites in the *Cyp2a5*-null allele and in the *Cyp2s1*-null allele were all oriented in the same direction. Mice of a *CMV-Cre* transgenic strain (B6.C-Tg (CMV-Cre)1Cgn/J, Stock 006054) were purchased from The Jackson Laboratory. In the *CMV-Cre* transgenic strain, deletion of loxP-flanked genes occurs in all tissues, including germ cells (Schwenk et al., 1995). The *Cre* gene in this strain is under the transcriptional control of a human cytomegalovirus minimal promoter and is likely to be expressed before implantation during early embryogenesis (Schwenk et al., 1995). All three mouse strains were on the B6 background.

Animals were bred by the following five steps (Fig. 2). First, *Cyp2s1*$^{-/-}$ strain was intercrossed with *Cyp2a5*$^{-/-}$ mice, yielding *Cyp2s1*$^{+/-}$/*Cyp2a5*$^{+/-}$ mice. Second, *Cyp2s1*$^{+/-}$/*Cyp2a5*$^{+/-}$ mice were crossed with B6 mice, and their pups were screened for both *Cyp2s1*$^{-}$ and *Cyp2a5*$^{-}$ alleles, using PCR (see Table 1 for primer sequences). Third, male *cis*-targeted *Cyp2s1*$^{+/-}$/*Cyp2a5*$^{+/-}$ mice were crossed with *CMV-Cre* females, and their pups were screened for the presence of the deleted allele (*Cyp2s1-Cyp2a5*$^{\Delta}$) by PCR, with the forward primer F1 located in the intron 3 of *Cyp2s1*, and reverse primer R1 at ~1 kb downstream of *Cyp2a5* exon 9 (Table 1). The PCR product from the *Cyp2s1-Cyp2a5*$^{\Delta}$ allele was validated by sequence analysis. Fourth, *Cyp2s1-Cyp2a5*$^{\Delta/+}$ mice were crossed with B6 mice, and *Cyp2s1-Cyp2a5*$^{\Delta/+}$ pups that were negative for the *Cre* transgene were identified. Fifth, *Cyp2s1-Cyp2a5*$^{\Delta/\Delta}$ homozygous mice were produced by intercrossing between *Cyp2s1-Cyp2a5*$^{\Delta/+}$ mice.

Characterization of the Cyp2s1-Cyp2a5$^{\Delta/\Delta}$ Mice. The absence of WT *Cyp2a4/5, Cyp2b10, Cyp2g1, and Cyp2s1* genes in the *Cyp2s1-Cyp2a5*$^{\Delta/\Delta}$ mice was confirmed by PCR, using primers shown in Table 1. Structure of the *Cyp2s1-Cyp2a5*$^{\Delta}$ allele was analyzed using Southern blot with two different probes: P1, a 846-bp fragment located ~3.3 kb downstream of *Cyp2a5* exon 9, and P2, a 817-bp fragment located in *Cyp2s1* intron 5, and ~2.2 kb upstream of the loxP site. Unless otherwise indicated, B6 mice were used as WT controls in all experiments described.

RNA-PCR Analysis. Tissues from 2-month-old male and female mice were pooled for RNA preparation. Total RNA from liver, lung, and nasal olfactory mucosa (OM) was isolated with use of the RNeasy Mini kit (QIAGEN, Valencia, CA), and was treated with DNase I (Invitrogen, Carlsbad, CA) before reverse transcription. RNA-PCR analysis was performed using a previously described protocol (Zhou et al., 2010) using gene-specific PCR primers for *Cyp2a4/5*, *Cyp2b9/10/19*, *Cyp2g1,* and glyceraldehyde 3-phosphate dehydrogenase (as an internal control) (Gu et al., 1999; Zhang et al., 2003). The gene-specific primers for *Cyp2s1* were 5′-gcgtggaacattggcaacgct-3′ and 5′-tggccccatggagagctgatcc-3′ (with an annealing temperature of 60°C), which amplify a 354-bp fragment corresponding to *Cyp2s1* exons 2–4.

Immunoblot Analysis. Microsomal preparation and immunoblot analysis were carried out essentially as described previously (Ding and Coon 1990; Zhang et al., 2009) using the following antibodies: goat anti-rat CYP1A1/2, rabbit anti-rat CYP3A2 (BD Gentest, Woburn, MA); rabbit anti-rat CYP2C, rabbit anti-rat cytochrome P450 reductase (CPR) (Enzo Life Science, Plymouth, PA); rabbit anti-human CYP2E1 (StressGen, Victoria, BC, Canada). Calnexin, a marker protein for the endoplasmic reticulum, was detected using a rabbit anti-human calnexin antibody (GenScript, Piscataway, NJ). The intensity of the detected bands was quantified with use of the Bio-Rad GS-710 Imaging Densitometer (Bio-Rad, Hercules, CA).

Histologic Analysis. Mice (2-month-old females and males) were euthanized by CO_2 overdose. Various tissues, including OM, brain, heart, thymus, lung, stomach, spleen, liver, pancreas, intestine, kidney, skin, and the reproductive organs, were fixed in 10% formalin and embedded in paraffin. Sections (4 μm thick) were stained with hematoxylin and eosin.

Determination of Microsomal P450 Activities. Liver, OM, lung, and brain microsomes were prepared from 2-month-old male mice using a protocol described previously (Ding and Coon, 1990). Microsomal testosterone metabolism was assayed essentially as previously described for OM (Zhou et al., 2009), liver (Zhou et al., 2010), and brain (Conroy et al., 2010). For lung, reaction mixtures contained 50 mM phosphate buffer (pH 7.4), 10 μM testosterone, 1 mM ascorbic acid, 1 mM NADPH, and 0.5 mg/ml microsomal protein and were incubated at 37°C for 30 minutes.

Testosterone metabolites were determined using a liquid chromatography-mass spectrometry (LC-MS) system consisting of an Agilent 1200 Series HPLC and an ABI 4000 Q-Trap mass spectrometer (Applied Biosystem, Foster City, CA), fitted with a 1.8-μm XDB-C18 column (4.6 × 50 mm; Agilent Technologies, Santa Clara, CA). The HPLC and MS conditions were as previously reported (Zhou et al., 2009, 2010; Conroy et al., 2010). Metabolites were identified by matching retention times and MS spectra with the authentic standards. The *m/z* values for the parent/product ions were 305/269 (for 2β-OH-, 6α-OH-, or 6β-OH-), 305/121 (for 11α-OH-), 305/97 (for 15α-OH-, 15β-OH-, or 16α-OH-), and 305/109 (for 16β-OH-T), and those for 16α-OH-progesterone (internal standard) were 331/97.

Other Methods. Pentobarbital clearance was assessed by a sleeping test (Tsuji et al., 1996), performed essentially as described previously (Wu et al., 2005). Protein concentration was determined by the bicinchoninic acid method (Pierce Chemical, Rockford, IL), using bovine serum albumin as the standard. Statistical analysis was carried out with GraphPad Prism 5 (GraphPad Software Inc., San Diego, CA). Statistical significance of differences between two groups was examined using Student's *t* test. Significance of differences in genotype distribution was analyzed with the χ^2 test.

Results

Generation and Characteristics of the Cyp2s1-Null Mouse. The strategy for targeted disruption of mouse *Cyp2s1* gene by homologous recombination in ES cells was to replace the exon 3 of *Cyp2s1* with a hygromycin-resistance gene, together with a loxP site (Fig. 1A). A positive ES cell clone (no. 55), with no random insertion of the targeting construct (as revealed by Southern blot analysis; data not shown) was used for blastocyst injection and generation of *Cyp2s1*-targeted chimeras. Three male chimeras were generated, two of which exhibited germline transmission, yielding F1 *Cyp2s1*$^{+/-}$ mice. The F1 heterozygotes, identified using PCR (Fig. 1B), were then intercrossed

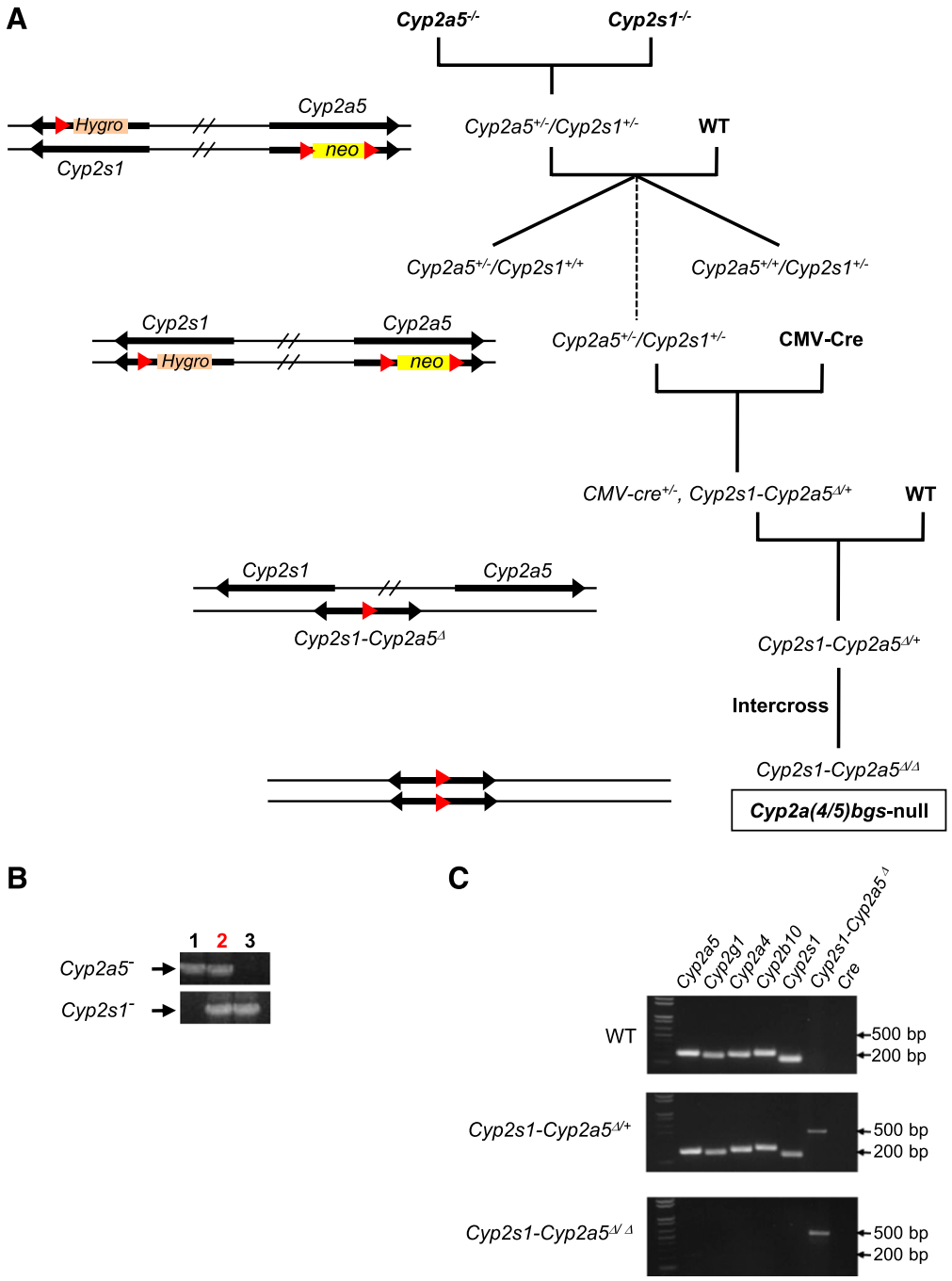

Fig. 2. Generation of the *Cyp2a(4/5)bgs*-null mouse model. (A) breeding strategy. (B) identification of the #28-2 pup as harboring the $Cyp2s1^{-}/Cyp2a5^{-}$ (double-knockout) allele. PCR detection of the $Cyp2s1^{-}$ and $Cyp2a5^{-}$ alleles was performed as described in methods. Representative $Cyp2s1^{+}/Cyp2a5^{-}$ (lane 1) and $Cyp2s1^{-}/Cyp2a5^{+}$ (lane 3) samples, and the sample for the #28-2 pup (lane 2), are shown. (C) characterization of the *Cyp2a(4/5)bgs*-null allele. Genomic DNA from WT, $Cyp2s1\text{-}Cyp2a5^{\Delta/+}$, and $Cyp2s1\text{-}Cyp2a5^{\Delta/\Delta}$ mice was analyzed, using PCR primers for *Cyp2a4*, *Cyp2a5*, *Cyp2g1*, *Cyp2b10*, *Cyp2s1*, $Cyp2s1\text{-}Cyp2a5^{\Delta}$, and *Cre*. Selected bands of a 100-bp DNA size marker are shown.

to generate F2 homozygous *Cyp2s1*-null ($Cyp2s1^{-/-}$) mice. On Southern blot analysis (Fig. 1C), the WT allele had a characteristic 7 kb band whereas the *Cyp2s1*-null allele showed an expected 10 kb band.

Pups derived from intercrosses between F1 heterozygotes showed Mendelian distribution of the three resultant genotypes (+/+, +/−, and −/−; data not shown), indicating absence of embryonic lethality. Homozygous *Cyp2s1*-null mice were indistinguishable from the WT littermates or WT B6 mice by their body weight, growth rate, organ weight, daily activity, or reproductive ability. Notably, $Cyp2s1^{-/-}$ males older than 10 months of age in early generations of the breeding colony were found to be infertile and had enlarged seminal vesicles (data not shown); however, these phenotypes appeared to be unrelated to CYP2S1 function, as they were not identified in similar mice of later generations.

Generation of the Cyp2a(4/5)bgs-null (Cyp2s1-Cyp2a5$^{\Delta/\Delta}$) Mouse. The $Cyp2s1\text{-}Cyp2a5^{\Delta/\Delta}$ mice were generated via an extensive, multigenerational breeding process that began with $Cyp2a5^{-/-}$ and

Cyp2s1$^{-/-}$ mice (Fig. 2). Given the short genomic distance between *Cyp2a5* and *Cyp2s1* (~1.2 Mb), the naturally occurring meiotic recombination event that would convert *trans*-targeted *Cyp2s1*$^{-}$ *and* *Cyp2a5*$^{-}$ alleles (i.e., alleles located on opposing chromosomes) to a *cis*-targeted configuration (i.e., on the same chromosome) was expected to be rare. Thus, 30 breeding pairs between *trans*-targeted *Cyp2s1*$^{+/-}$/*Cyp2a5*$^{+/-}$ mice and WT mice were coordinated, of which 28 pairs were fertile and gave birth to a total of 170 pups. In the absence of the desired meiotic recombination, the pups would be positive for only the *Cyp2a5*$^{-}$ or the *Cyp2s1*$^{-}$ allele, but not both, which was the case for all but one (#28-2) of the 170 pups analyzed. The #28-2 pup, hereafter named *cis*-targeted *Cyp2s1*$^{+/-}$/*Cyp2a5*$^{+/-}$ mouse, was identified to have both *Cyp2s1*$^{-}$ and *Cyp2a5*$^{-}$ alleles (Fig. 2B). The apparent recombination ratio between *Cyp2s1* and *Cyp2a5* genes was calculated to be ~0.6% (1 in 170).

The *cis*-targeted *Cyp2s1*$^{+/-}$/*Cyp2a5*$^{+/-}$ mice were crossed with *CMV-Cre* mice for deletion of the 1.2-Mb floxed region harboring nine *Cyp* genes, including, sequentially, *Cyp2a5, 2g1, 2b19, 2b23, 2a4, 2b9, 2b13, 2b10,* and *2s1*. The *CMV-Cre* transgene was located on the X chromosome. To increase breeding efficiency, *CMV-Cre* females, with two copies of Chr X, were crossed to *cis*-targeted *Cyp2s1*$^{+/-}$/*Cyp2a5*$^{+/-}$ males. Among the *CMV-Cre*$^{+/-}$/*Cyp2s1*$^{+/-}$/*Cyp2a5*$^{+/-}$ pups, those harboring the *Cyp2s1-Cyp2a5*$^{\Delta}$ allele in their tail DNA, identified by PCR analysis (Fig. 2C), were crossed with WT mice again to identify those with germline transmission of the *Cyp2s1-Cyp2a5*$^{\Delta}$ allele and were also negative for the *CMV-Cre* transgene. *Cyp2s1-Cyp2a5*$^{\Delta/\Delta}$ homozygotes were then generated via intercrosses between heterozygotes. Successful deletion of the gene cluster was confirmed by PCR using primers for representative members, including *Cyp2a4/5*, *Cyp2b10*, *Cyp2g1*, and *Cyp2s1*, for which characteristic PCR products were detected in the genomic DNA of WT mice but not in the *Cyp2s1-Cyp2a5*$^{\Delta/\Delta}$ mice (Fig. 2C). The deletion of *Cyp2a(4/5)bgs* gene cluster was also confirmed by Southern blot analysis (Fig. 3B), which showed characteristic bands of 9.6 kb and 3.1 kb for the WT allele and a band of 6.6 kb for the *Cyp2s1-Cyp2a5*$^{\Delta}$ allele; analysis by RNA-PCR showed absence of CYP2A4/5, CYP2B9/10/19, CYP2G1, and CYP2S1 mRNAs in the *Cyp2s1-Cyp2a5*$^{\Delta/\Delta}$ mice (Fig. 3C).

General Characteristics of the Cyp2a(4/5)bgs-Null Mouse. Homozygous *Cyp2a(4/5)bgs*-null mice were found to be viable and fertile. The pups derived from intercrosses between *Cyp2a(4/5)bgs*-null heterozygotes consisted of 24% (21 of 88) homozygotes, 44% (39 of 88) heterozygotes, and 32% (28 of 88) WT littermates. The profile of genotype distribution was not significantly different from that (25%, 50%, 25%) predicted by Mendelian distribution ($P > 0.05$, χ^2 test), suggesting absence of embryonic lethality. The body and organ weights (liver, kidney, lung, brain, testis, and heart for males, and liver, kidney, lung, brain, and heart for females) were similar between null and WT mice at 2 months of age (Table 2), indicating normal growth of the null mice. Histologic analyses of various tissues,

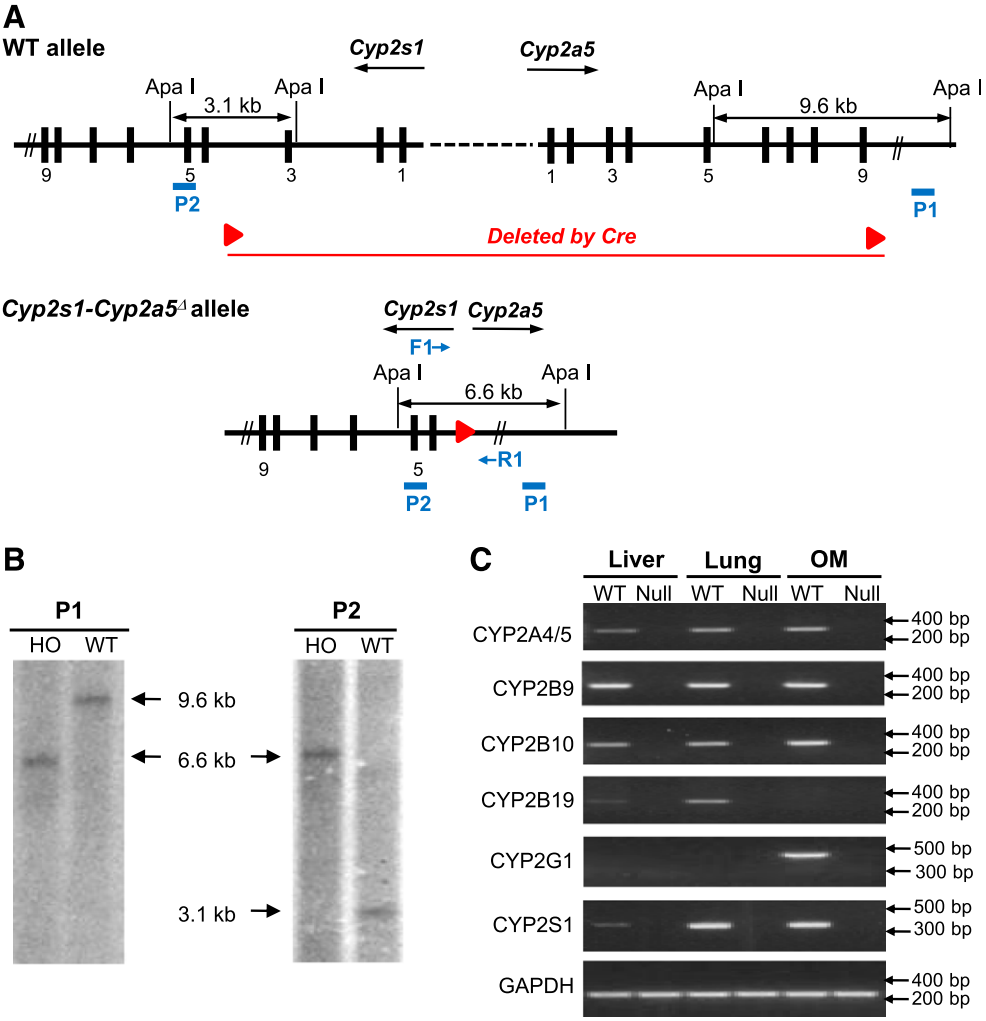

Fig. 3. Confirmation of gene cluster deletion in the *Cyp2a(4/5)bgs*-null (*Cyp2s1-Cyp2a5*$^{\Delta/\Delta}$) mice. (A) strategy of Southern blot analysis. DNA probes P1 and P2 are shown as blue bars. Genomic DNA was digested by Apa I. Probe P1 would detect a 9.6-kb fragment from *Cyp2a5* WT allele, whereas probe P2 would detect a 3.1-kb fragment from *Cyp2s1* WT allele; both probes would detect a 6.6-kb fragment from the *Cyp2s1-Cyp2a5*$^{\Delta}$ allele. (B) Southern blot analysis of WT and *Cyp2s1-Cyp2a5*$^{\Delta/\Delta}$ (HO) mice. Ten micrograms of genomic DNA were used for each lane. (C) RNA-PCR analysis of CYP2A4/5, CYP2B9/10/19, CYP2G1, and CYP2S1 expression in liver, lung, and OM of WT and *Cyp2a(4/5)bgs*-null mice. Tissues from 2-month-old (one male and one female) mice were pooled for total RNA preparation. PCR products were analyzed on a 1.5% agarose gel, and visualized by staining with ethidium bromide. The positions of selected fragments of a 100-bp DNA marker are indicated.

TABLE 2

Body and tissue weights of WT and Cyp2a(4/5)bgs-null mice

The body and organ weights were determined at 2 months of age. Values presented are means ± S.D. (n = 6). There was no significant difference between WT and null mice in either sex ($P > 0.05$).

Mouse	Body Weight	Tissue Weight					
		Liver	Lung	Kidney	Heart	Brain	Testis
	g	*g*					
WT, male	24.5 ± 0.9	1.38 ± 0.02	0.16 ± 0.03	0.34 ± 0.02	0.11 ± 0.01	0.34 ± 0.01	0.17 ± 0.02
Null, male	24.7 ± 1.3	1.37 ± 0.06	0.16 ± 0.02	0.35 ± 0.02	0.11 ± 0.01	0.35 ± 0.02	0.18 ± 0.01
WT, female	20.9 ± 0.6	1.09 ± 0.06	0.12 ± 0.01	0.24 ± 0.02	0.10 ± 0.01	0.30 ± 0.01	N/A
Null, female	20.5 ± 0.8	1.03 ± 0.05	0.12 ± 0.01	0.23 ± 0.02	0.10 ± 0.01	0.30 ± 0.01	N/A

N/A, not applicable; WT, wild type.

including OM, brain, heart, thymus, lung, stomach, spleen, liver, pancreas, intestine, kidney, skin, and the reproductive organs, revealed no obvious abnormalities (data not shown). Additionally, despite the loss of nine *Cyp2* genes, the expression of CPR and various other P450 enzymes, including CYP2C, CYP3A, CYP2E1, and CYP1A1/2, was similar to that in WT mice in the lung, OM, and liver of both males (Fig. 4) and females (data not shown), indicating no significant compensatory changes.

Impact of the Loss of the Cyp2a(4/5)bgs Gene Cluster on Microsomal P450 Activities In Vitro and Drug Metabolism In Vivo. As shown in Table 3, differences in rates of metabolism of testosterone between the *Cyp2a(4/5)bgs*-null and WT mice were found for all four tissues examined (liver, lung, OM, and brain). The major metabolites, as previously described for each tissue (Zhou et al., 2009, 2010; Conroy et al., 2010), were detected and quantified. In the lung and OM, three major metabolites produced in the WT mice (15α-OH-T, 15β-OH-T and 2β-OH-T) were barely detected in the null mice. In the liver, an ~50% decrease was found in rates of formation of 15β-OH-T. In the brain, one of the major metabolites, 16α-OH-T, was found to be formed at ~40% lower rates in the null mice compared with WT mice. These results indicated that the P450s encoded by this *Cyp2* gene cluster, which are preferentially expressed in the respiratory tract, play an important role in OM and lung microsomal activities toward testosterone metabolism, whereas members of the gene cluster also contribute to testosterone metabolism in brain and liver.

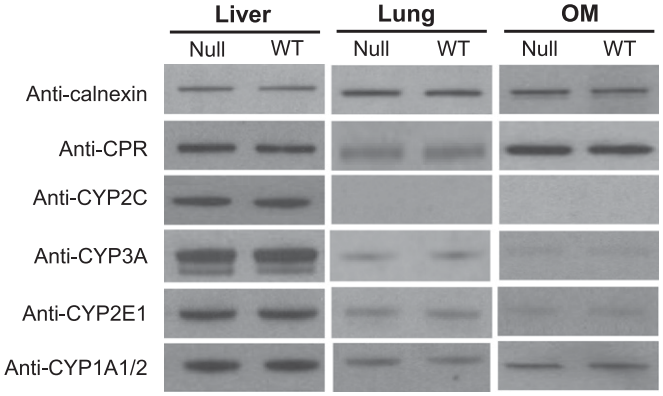

Fig. 4. Immunoblot analysis of the expression of selected P450 and CPR. Microsomes were prepared from pooled liver, lung, or OM of WT and *Cyp2a(4/5)bgs*-null (Null) male mice (five per group, 2 months old). Microsomal proteins from the liver (5 μg per lane), lung, and OM (10 μg per lane) were analyzed for the expression of selected P450 or CPR proteins. The expression of calnexin was analyzed as a loading control. The antibodies used are described in *Materials and Methods*. Densitometric analysis (not shown) for each panel indicated that the maximal difference in band intensity between samples from WT and Null mice was less than 20%. Similar results were obtained in female mice (data not shown).

The impact of loss of *Cyp2a(4/5)bgs* gene cluster on systemic drug clearance was examined, with use of pentobarbital as an example. Rates of pentobarbital clearance were determined by a sleeping test in which the length of sleeping time after drug administration is inversely related to the rate of drug metabolism. At a dose of pentobarbital of 60 mg/kg i.p., pentobarbital-induced sleep time was significantly longer (>60%) in *Cyp2a(4/5)bgs*-null than in WT mice (Table 4), indicating that members of this gene cluster play a significant role in pentobarbital clearance in vivo.

Discussion

To the best of our knowledge, this is the first time a knockout mouse with *Cre*-mediated megabase gene deletion was generated using the "in vivo" approach, either with the targeted meiotic recombination (TAMERE) (Herault et al., 1998) or the sequential targeted recombination-induced genomic (STRING) method (Spitz et al., 2005). In the TAMERE method, the Cre recombinase acts on two loxP sites in a *trans* configuration; in the STRING method, the Cre recombinase acts on two loxP sites in a *cis* configuration (as was done here). In the original study by Spitz et al., Cre-mediated inversion of large (3- and 7-Mb) genomic fragments at the *Itga6*, *Hoxd*, and *Cd44* loci on mouse Chr 2 was successful, but Cre-mediated deletion of these same fragments did not lead to viable newborns, presumably due to early embryonic lethality (Spitz et al., 2005). A failed attempt to use the TAMERE method to delete a 3.9-Mb region on mouse Chr 16 was also reported, leading to the conclusion that in vitro approach is more efficient than is the in vivo approach for long-range chromosomal engineering (Olson et al., 2005).

In the present study, our attempts at the in vitro approach were unsuccessful (data not shown), presumably because of our use of the B6-derived Bruce4 ES cell line. We chose to make the *Cyp2a(4/5)bgs*-null mouse on the B6 background, given the intended utility of the mouse model for drug metabolism and toxicology studies. However, B6-derived ES cells appeared to be less amenable than the commonly used 129/Sv or FVB ES cells to the multiple rounds of electroporation/selection that are required by the in vitro targeting approach. These cells, however, were adequate for generation of *Cyp2a5-null* and *Cyp2s1*-null mice, which were used to produce the *Cyp2a(4/5)bgs*-null mouse. Thus, our results demonstrate that it is possible to generate mouse models with megabase-sized gene deletion using the STRING method, and they suggest that the in vivo approach may be preferable for generation of megabase gene-deletion mouse models on the B6 background.

In the *Cyp2a(4/5)bgs* gene cluster, besides the nine targeted full-length *Cyp2* genes, there are five full-length, non-*Cyp* genes (NCBI mouse genome map, Build-38.1): *Vmn1r184*, *Nalp9c*, *Nalp4a*,

TABLE 3

In vitro metabolism of testosterone

Liver, lung, OM, and brain microsomes were prepared from 2-month-old male WT and Cyp2a(4/5)bgs-null mice. Reaction mixtures contained 50 mM phosphate buffer, pH 7.4, 10 μM testosterone, 1 mM ascorbic acid, 1 mM NADPH, and 0.1 mg/ml (for OM and liver) or 0.5 mg/ml (for lung and brain) microsomal protein. The values presented are means ± S.D. (n = 3).

Tissue	Genotype	Rates of Product Formation							
		15α-OH-T	15β-OH-T	2β-OH-T	16α-OH-T	16β-OH-T	6α-OH-T	6β-OH-T	11α-OH-T
		pmol/min/mg protein							
Lung	WT	80 ± 5	3 ± 1	4 ± 1	30 ± 6	7 ± 2	<0.02[a]	<0.02	<0.02
	Null	3 ± 0[b]	<0.01	<0.01	30 ± 7	2 ± 1[b]	<0.02	<0.02	<0.02
OM	WT	4100 ± 200	320 ± 60	380 ± 50	<0.5	<0.1	<0.2	<0.2	<0.2
	Null	<0.1	<0.1	<0.1	<0.5	<0.1	<0.2	<0.2	<0.2
Brain	WT	0.16 ± 0.03	<0.01	<0.01	0.14 ± 0.03	0.03 ± 0.01	0.04 ± 0.01	<0.01	0.02 ± 0.00
	Null	0.14 ± 0.03	<0.01	<0.01	0.08 ± 0.03[b]	0.03 ± 0.01	0.04 ± 0.01	<0.01	0.02 ± 0.00
			15β-OH-T		16α-OH-T			6β-OH-T	
Liver[c]	WT		5.6 ± 1.2		260 ± 20			120 ± 30	
	Null		2.3 ± 0.1[b]		250 ± 30			120 ± 20	

OM, nasal olfactory mucosa; WT, wild type.
[a]Estimated on the basis of detection limits, which were respectively 0.02 (15α-OH-T), 0.01 (15β-OH-T), 0.07 (2β-OH-T), 0.02 (16α-OH-T), 0.01 (16β-OH-T), and 0.03 (6α-OH-T, 6β-OH-T, and 11α-OH-T) pmol on column.
[b]Significantly lower than the corresponding WT value, $P < 0.01$ (Student's t test).
[c]Only previously reported major metabolites were determined (Zhou et al., 2010).

Nalp9a, and *Vmn1r185*. Our finding that *Cyp2a(4/5)bgs*-null mice are viable and fertile indicates that these five non-*Cyp* genes are not critical for embryonic or postnatal development or for reproduction. The *Nalp4* and *Nalp9* (also named *Nlrp4* and *Nlrp9*) genes are members of the *NLRP* (nucleotide-binding oligomerization domain, leucine-rich repeat, and pyrin domain–containing proteins) gene family (Tian et al., 2009), which are mainly expressed in oocytes and embryos in early developmental stages. The availability of the *Cyp2a(4/5)bgs*-null mouse, as a *Nlrp9c-4a-9a* knockout mouse, may be helpful for studies on potential compensatory mechanisms in the oocyte, and on other potential biologic functions of these proteins. The two *Vmn1r* (also named *V1r*) genes are members of mouse vomeronasal 1 receptor gene superfamily, which encodes rodent pheromone receptors expressed by vomeronasal sensory neurons (Ryba and Tirindelli, 1997). Little is known regarding the expression or property of *Vmn1r184* and *Vmn1r185*; the *Cyp2a(4/5)bgs*-null mouse may thus be useful for studying their potential chemosensory functions. Notably, the deletion of these five non-*Cyp* genes is not expected to have any effect on drug metabolism and biotransformation.

The nine full-length *Cyp* genes that are deleted in the *Cyp2a(4/5)bgs-null* mouse include all five *Cyp2b* genes (Wang, et al., 2003) and the two major *Cyp2a* genes involved in xenobiotic metabolism (Su and Ding, 2004). This feature makes the *Cyp2a(4/5)bgs-null* mouse very useful, not only for determination of the combined functions of these mouse P450s in various tissues, but also for production of humanized mouse models that express the human CYP2A/2B/2S enzymes. In that regard, the orthologous human CYP2A (2A6 and 2A13) and CYP2B (2B6) genes are expressed in liver and various extrahepatic tissues, and the encoded enzymes are active toward numerous xenobiotic compounds (Raunio et al., 2008; Ding and Kaminsky, 2003; Wang and Tompkins, 2008). Transgenic mouse models expressing either human CYP2A6 (Zhang et al., 2005) or CYP2A13/CYP2B6 (Wei et al., 2012) are already available, which can be used for crossbreeding with the null mice. Additionally, given the fact that *Cyp2b10* is a major target gene of the constitutive androstane receptor, the new mouse model will be useful for assessing whether the expression and regulation of *Cyp2b10* have a role in accounting for the diverse functions of this receptor.

Of the other two targeted mouse *Cyp* genes (*2g1* and *2s1*), *Cyp2g1* is known to encode a functional enzyme. In mice and several other mammalian species, CYP2G1 is uniquely expressed in OM, and mouse CYP2G1 has been found to be active toward both endogenous (e.g., testosterone) and exogenous substrates (e.g., the olfactory toxicant dichlobenil) (Hua et al., 1997; Gu et al., 1998 Zhuo et al., 2004). However, humans no longer have a functional *CYP2G* gene (Sheng et al., 2000).

CYP2S1 is mainly expressed in extrahepatic tissues in mice and humans (Saarikoski et al., 2005). The activity of mouse CYP2S1 has not been examined. The activity of recombinant human CYP2S1 has been studied in several laboratories (e.g., Smith et al., 2003; Karlgren et al., 2005; Wang et al., 2005; Wu et al., 2006). Although the results from these studies were sometimes conflicting, CYP2S1 appears to have limited ability in vitro to catalyze NADPH-dependent oxidative metabolism (e.g., Wu et al., 2006); however, it is effective in catalyzing NADPH-independent, hydroperoxide or lipid peroxide-supported oxidation of many xenobiotic and endogenous compounds (Bui et al., 2009, 2011). Furthermore, CYP2S1 could be reduced by P450 reductase and is efficient in metabolizing certain drugs in an NADPH-dependent fashion under hypoxic conditions (Nishida et al., 2010; Xiao et al., 2011). Nonetheless, it remains to be determined whether CYP2S1 plays any biologic function, or to what extent it can contribute to xenobiotic metabolism, in vivo. Our newly generated *Cyp2s1*-null mouse should be valuable for addressing these questions. In that regard, the fact that *Cyp2s1*-null mice are viable and fertile indicates that CYP2S1 is not critical for embryonic or postnatal development or for reproduction.

TABLE 4

Pentobarbital-induced sleeping time in WT and Cyp2a(4/5)bgs-null (null) mice

Adult male and female mice (four in each group; 2 to 3 months old) were treated with pentobarbital (in phosphate-buffered saline) at a dose of 60 mg/kg i.p. The lengths of time between drug administration and the loss and the subsequent recovery of righting reflex were recorded. Values presented are means ± S.D.

Mouse	Sleep Latency	Sleep Time
	min	
WT, male	4.3 ± 0.4	51 ± 5
Null, male	4.2 ± 0.5	90 ± 12[a]
WT, female	4.0 ± 0.5	53 ± 8
Null, female	4.1 ± 0.6	85 ± 8[a]

WT, wild type.
[a] Significantly greater than the WT group, $P < 0.01$ (Student's t test).

Testosterone is a known substrate for multiple P450 enzymes. The roles of CYP2A5/2G1 in testosterone hydroxylation in OM (Zhuo et al., 2004) and the role of CYP2A5 in testosterone hydroxylation in liver (Zhou et al., 2010) and lateral nasal gland (Zhou et al., 2011) have been studied previously using *Cyp2a5*-null and *Cyp2g1*-null mice, but the contributions of the CYP2A(4/5)BGS enzymes to testosterone metabolism in the lung and brain have not been examined until now. Our results showed that, in the lung, they play an important role in the formation of 15α-OH-T (the most abundant metabolite detected in lung), 15β-OH-T, 2β-OH-T [presumably all formed by CYP2A5 (Zhou et al., 2011)], and 16β-OH-T [presumably formed by CYP2B (Sonderfan et al., 1987)]; these enzymes do not appear to play a role, however, in the formation of 16α-OH-T [preferentially formed by CYP2D9 (Ichikawa et al., 1989)]. The overall rates of testosterone metabolism in the brain were much lower than those in the other tissues examined, but multiple metabolites were detected. One of these, 16α-OH-T, was found with a significant decrease in rate of formation (40%) in the null mice. Thus, one or more of the targeted *Cyp* genes in the *Cyp2a(4/5)bgs*-null mouse are functional as a testosterone 16α-hydroxylase in the brain; the most likely candidates are the *Cyp2b* genes, given the known expression and drug-metabolizing activity of CYP2B enzymes in the brain (Ferguson and Tyndale, 2011). Conversely, our data also suggested that the other testosterone metabolites formed by brain microsomes (15α-OH-T, 16β-OH-T, 6α-OH-T, and 11α-OH-T) were not formed by any of the nine targeted CYP2 enzymes.

The specific P450 enzymes involved in the systemic clearance of pentobarbital in mice have not been determined previously. On the basis of results from the pentobarbital sleeping test, we conclude that one or more of the targeted P450s in the *Cyp2a(4/5)bgs*-null mouse play a significant role in pentobarbital clearance in vivo. However, by comparing the extent of increase in pentobarbital-sleeping time seen in the *Cyp2a(4/5)bgs*-null mouse ($\sim$2-fold) with those seen previously in the liver-*Cpr*-null mouse in which all hepatic microsomal P450 enzymes were inactivated [$>$10-fold (Gu et al., 2003)], we can further conclude that other P450 enzymes also make important contributions to pentobarbital clearance.

In summary, we have generated a novel *Cyp2a(4/5)bgs* gene cluster-null mouse via in vivo chromosome engineering. Our study demonstrates the utility of the STRING approach for generating mouse models with deletion of a megabase-sized gene fragment. The *Cyp2a(4/5)bgs*-null mice, which are viable and fertile without any obvious abnormalities, will be useful for functional analysis of the nine targeted full-length *Cyp* genes in xenobiotic metabolism and chemical toxicity in various tissues where one or more of the targeted *Cyp* genes are known to be expressed in WT mice, including the liver, lung, brain, intestine, kidney, skin, and OM. The generation of the *Cyp2a(4/5)bgs*-null mouse model also paves the way for the preparation of humanized mouse models that express the orthologous human *CYP2A*, *2B6*, and *2S1* genes.

Acknowledgments

The authors gratefully acknowledge the use of the Biochemistry, Molecular Genetics, and Transgenic and Knockout Mouse Core facilities of the Wadsworth Center, New York State Department of Health. The authors thank Dr. Fang Xie for assistance with LC-MS/MS.

Authorship Contributions

Participated in research design: Wei, Li, Zhou, Zhang, Kluetzman, Ding.

Conducted experiments: Wei, Li, Zhou, Zhang, Dunbar, Liu, Kluetzman, Yang.

Performed data analysis: Wei, Li, Liu, Yang, Ding.

Wrote or contributed to the writing of the manuscript: Wei, Li, Zhang, Liu, Ding.

References

Bui P, Imaizumi S, Beedanagari SR, Reddy ST, and Hankinson O (2011) Human CYP2S1 metabolizes cyclooxygenase- and lipoxygenase-derived eicosanoids. *Drug Metab Dispos* **39**: 180–190.

Bui PH, Hsu EL, and Hankinson O (2009) Fatty acid hydroperoxides support cytochrome P450 2S1-mediated bioactivation of benzo[a]pyrene-7,8-dihydrodiol. *Mol Pharmacol* **76**: 1044–1052.

Brault V, Pereira P, Duchon A, and Hérault Y (2006) Modeling chromosomes in mouse to explore the function of genes, genomic disorders, and chromosomal organization. *PLoS Genet* **2**:e86.

Conroy JL, Fang C, Gu J, Zeitlin SO, Yang W, Yang J, VanAlstine MA, Nalwalk JW, Albrecht PJ, Mazurkiewicz JE, et al. (2010) Opioids activate brain analgesic circuits through cytochrome P450/epoxygenase signaling. *Nat Neurosci* **13**:284–286.

Damiri B, Holle E, Yu X, and Baldwin WS (2012) Lentiviral-mediated RNAi knockdown yields a novel mouse model for studying Cyp2b function. *Toxicol Sci* **125**:368–381.

Ding X and Coon MJ (1994) Steroid metabolism by rabbit olfactory-specific P450 2G1. *Arch Biochem Biophys* **315**:454–459.

Ding X and Kaminsky LS (2003) Human extrahepatic cytochromes P450: function in xenobiotic metabolism and tissue-selective chemical toxicity in the respiratory and gastrointestinal tracts. *Annu Rev Pharmacol Toxicol* **43**:149–173.

Ding XX and Coon MJ (1990) Immunochemical characterization of multiple forms of cytochrome P-450 in rabbit nasal microsomes and evidence for tissue-specific expression of P-450s NMa and NMb. *Mol Pharmacol* **37**:489–496.

Ferguson CS and Tyndale RF (2011) Cytochrome P450 enzymes in the brain: emerging evidence of biological significance. *Trends Pharmacol Sci* **32**:708–714.

Gonzalez FJ (2003) Role of gene knockout and transgenic mice in the study of xenobiotic metabolism. *Drug Metab Rev* **35**:319–335.

Gu J, Cui H, Behr M, Zhang L, Zhang QY, Yang W, Hinson JA, and Ding X (2005) In vivo mechanisms of tissue-selective drug toxicity: effects of liver-specific knockout of the NADPH-cytochrome P450 reductase gene on acetaminophen toxicity in kidney, lung, and nasal mucosa. *Mol Pharmacol* **67**:623–630.

Gu J, Dudley C, Su T, Spink DC, Zhang QY, Moss RL, and Ding X (1999) Cytochrome P450 and steroid hydroxylase activity in mouse olfactory and vomeronasal mucosa. *Biochem Biophys Res Commun* **266**:262–267.

Gu J, Weng Y, Zhang QY, Cui H, Behr M, Wu L, Yang W, Zhang L, and Ding X (2003) Liver-specific deletion of the NADPH-cytochrome P450 reductase gene: impact on plasma cholesterol homeostasis and the function and regulation of microsomal cytochrome P450 and heme oxygenase. *J Biol Chem* **278**:25895–25901.

Gu J, Zhang QY, Genter MB, Lipinskas TW, Negishi M, Nebert DW, and Ding X (1998) Purification and characterization of heterologously expressed mouse CYP2A5 and CYP2G1: role in metabolic activation of acetaminophen and 2,6-dichlorobenzonitrile in mouse olfactory mucosal microsomes. *J Pharmacol Exp Ther* **285**:1287–1295.

Hérault Y, Rassoulzadegan M, Cuzin F, and Duboule D (1998) Engineering chromosomes in mice through targeted meiotic recombination (TAMERE). *Nat Genet* **20**:381–384.

Hoffman SM, Nelson DR, and Keeney DS (2001) Organization, structure and evolution of the CYP2 gene cluster on human chromosome 19. *Pharmacogenetics* **11**:687–698.

Hua Z, Zhang QY, Su T, Lipinskas TW, and Ding X (1997) cDNA cloning, heterologous expression, and characterization of mouse CYP2G1, an olfactory-specific steroid hydroxylase. *Arch Biochem Biophys* **340**:208–214.

Ichikawa T, Itakura T, and Negishi M (1989) Functional characterization of two cytochrome P-450s within the mouse, male-specific steroid 16 alpha-hydroxylase gene family: expression in mammalian cells and chimeric proteins. *Biochemistry* **28**:4779–4784.

Johnson KA, Lerner CP, Di Lacio LC, Laird PW, Sharpe AH, and Simpson EM (1995) Transgenic mice for the preparation of hygromycin-resistant primary embryonic fibroblast feeder layers for embryonic stem cell selections. *Nucleic Acids Res* **23**:1273–1275.

Karlgren M, Miura S, and Ingelman-Sundberg M (2005) Novel extrahepatic cytochrome P450s. *Toxicol Appl Pharmacol* **207**(Suppl 2)57–61.

Köntgen F, Süss G, Stewart C, Steinmetz M, and Bluethmann H (1993) Targeted disruption of the MHC class II Aa gene in C57BL/6 mice. *Int Immunol* **5**:957–964.

Li L, Wei Y, Van Winkle L, Zhang QY, Zhou X, Hu J, Xie F, Kluetzman K, and Ding X (2011) Generation and characterization of a *Cyp2f2*-null mouse and studies on the role of CYP2F2 in naphthalene-induced toxicity in the lung and nasal olfactory mucosa. *J Pharmacol Exp Ther* **339**:62–71.

Nagy A (2000) Cre recombinase: the universal reagent for genome tailoring. *Genesis* **26**:99–109.

Nishida CR, Lee M, and de Montellano PR (2010) Efficient hypoxic activation of the anticancer agent AQ4N by CYP2S1 and CYP2W1. *Mol Pharmacol* **78**:497–502.

Olson LE, Tien J, South S, and Reeves RH (2005) Long-range chromosomal engineering is more efficient in vitro than in vivo. *Transgenic Res* **14**:325–332.

Raunio H, Hakkola J, and Pelkonen O (2008) The CYP2A subfamily, in *Cytochrome P450: Role in the Metabolism and Toxicity of Drugs and Other Xenobiotics* (Ioannides C, ed), pp 150–177, RSC Publishing, Cambridge, UK.

Ryba NJ and Tirindelli R (1997) A new multigene family of putative pheromone receptors. *Neuron* **19**:371–379.

Saarikoski ST, Wikman HA, Smith G, Wolff CH, and Husgafvel-Pursiainen K (2005) Localization of cytochrome P450 CYP2S1 expression in human tissues by in situ hybridization and immunohistochemistry. *J Histochem Cytochem* **53**:549–556.

Scheer N, Kapelyukh Y, McEwan J, Beuger V, Stanley LA, Rode A, and Wolf CR (2012) Modeling human cytochrome P450 2D6 metabolism and drug-drug interaction by a novel panel of knockout and humanized mouse lines. *Mol Pharmacol* **81**:63–72.

Schwenk F, Baron U, and Rajewsky K (1995) A cre-transgenic mouse strain for the ubiquitous deletion of loxP-flanked gene segments including deletion in germ cells. *Nucleic Acids Res* **23**: 5080–5081.

Sheng J, Guo J, Hua Z, Caggana M, and Ding X (2000) Characterization of human CYP2G genes: widespread loss-of-function mutations and genetic polymorphism. *Pharmacogenetics* **10**:667–678.

Smith G, Wolf CR, Deeni YY, Dawe RS, Evans AT, Comrie MM, Ferguson J, and Ibbotson SH (2003) Cutaneous expression of cytochrome P450 CYP2S1: individuality in regulation by therapeutic agents for psoriasis and other skin diseases. *Lancet* **361**:1336–1343.

Sonderfan AJ, Arlotto MP, Dutton DR, McMillen SK, and Parkinson A (1987) Regulation of testosterone hydroxylation by rat liver microsomal cytochrome P-450. *Arch Biochem Biophys* **255**:27–41.

Spitz F, Herkenne C, Morris MA, and Duboule D (2005) Inversion-induced disruption of the Hoxd cluster leads to the partition of regulatory landscapes. *Nat Genet* **37**:889–893.

Su T and Ding X (2004) Regulation of the cytochrome P450 2A genes. *Toxicol Appl Pharmacol* **199**:285–294.

Tian X, Pascal G, and Monget P (2009) Evolution and functional divergence of NLRP genes in mammalian reproductive systems. *BMC Evol Biol* **9**:202.

Tsuji R, Isobe N, and Kawasaki H (1996) Mechanism of prolongation of pentobarbital-induced sleeping time by empenthrin in mice. *Toxicology* **108**:185–190.

van Herwaarden AE, Wagenaar E, van der Kruijssen CM, van Waterschoot RA, Smit JW, Song JY, van der Valk MA, van Tellingen O, van der Hoorn JW, Rosing H, et al. (2007) Knockout of cytochrome P450 3A yields new mouse models for understanding xenobiotic metabolism. *J Clin Invest* **117**:3583–3592.

Wang H, Donley KM, Keeney DS, and Hoffman SM (2003) Organization and evolution of the Cyp2 gene cluster on mouse chromosome 7, and comparison with the syntenic human cluster. *Environ Health Perspect* **111**:1835–1842.

Wang H and Tompkins LM (2008) CYP2B6: new insights into a historically overlooked cytochrome P450 isozyme. *Curr Drug Metab* **9**:598–610.

Wang SL, He XY, and Hong JY (2005) Human cytochrome p450 2s1: lack of activity in the metabolic activation of several cigarette smoke carcinogens and in the metabolism of nicotine. *Drug Metab Dispos* **33**:336–340.

Wei Y, Wu H, Li L, Liu Z, Zhou X, Zhang QY, Weng Y, D'Agostino J, Ling G, Zhang X, et al. (2012) Generation and characterization of a CYP2A13/2B6/2F1-transgenic mouse model. *Drug Metab Dispos* **40**:1144–1150.

Wei Y, Zhou X, Fang C, Li L, Kluetzman K, Yang W, Zhang QY, and Ding X (2010) Generation of a mouse model with a reversible hypomorphic cytochrome P450 reductase gene: utility for tissue-specific rescue of the reductase expression, and insights from a resultant mouse model with global suppression of P450 reductase expression in extrahepatic tissues. *J Pharmacol Exp Ther* **334**:69–77.

Weng Y, Fang C, Turesky RJ, Behr M, Kaminsky LS, and Ding X (2007) Determination of the role of target tissue metabolism in lung carcinogenesis using conditional cytochrome P450 reductase-null mice. *Cancer Res* **67**:7825–7832.

Wu L, Gu J, Cui H, Zhang QY, Behr M, Fang C, Weng Y, Kluetzman K, Swiatek PJ, Yang W, et al. (2005) Transgenic mice with a hypomorphic NADPH-cytochrome P450 reductase gene: effects on development, reproduction, and microsomal cytochrome P450. *J Pharmacol Exp Ther* **312**:35–43.

Wu ZL, Sohl CD, Shimada T, and Guengerich FP (2006) Recombinant enzymes overexpressed in bacteria show broad catalytic specificity of human cytochrome P450 2W1 and limited activity of human cytochrome P450 2S1. *Mol Pharmacol* **69**:2007–2014.

Xiao Y, Shinkyo R, and Guengerich FP (2011) Cytochrome P450 2S1 is reduced by NADPH-cytochrome P450 reductase. *Drug Metab Dispos* **39**:944–946.

Xie F, Zhou X, Behr M, Fang C, Horii Y, Gu J, Kannan K, and Ding X (2010) Mechanisms of olfactory toxicity of the herbicide 2,6-dichlorobenzonitrile: essential roles of CYP2A5 and target-tissue metabolic activation. *Toxicol Appl Pharmacol* **249**:101–106.

Xie F, Zhou X, Genter MB, Behr M, Gu J, and Ding X (2011) The tissue-specific toxicity of methimazole in the mouse olfactory mucosa is partly mediated through target-tissue metabolic activation by CYP2A5. *Drug Metab Dispos* **39**:947–951.

Yu Y and Bradley A (2001) Engineering chromosomal rearrangements in mice. *Nat Rev Genet* **2**: 780–790.

Zhang QY, Dunbar D, and Kaminsky LS (2003) Characterization of mouse small intestinal cytochrome P450 expression. *Drug Metab Dispos* **31**:1346–1351.

Zhang QY, Fang C, Zhang J, Dunbar D, Kaminsky L, and Ding X (2009) An intestinal epithelium-specific cytochrome P450 (P450) reductase-knockout mouse model: direct evidence for a role of intestinal p450s in first-pass clearance of oral nifedipine. *Drug Metab Dispos* **37**:651–657.

Zhang QY, Gu J, Su T, Cui H, Zhang X, D'Agostino J, Zhuo X, Yang W, Swiatek PJ, and Ding X (2005) Generation and characterization of a transgenic mouse model with hepatic expression of human CYP2A6. *Biochem Biophys Res Commun* **338**:318–324.

Zhang QY and Ding X (2008) The CYP2F, CYP2G and CYP2J subfamilies, in *Cytochrome P450: Role in the Metabolism and Toxicity of Drugs and Other Xenobiotics* (Ioannides C, ed), pp 309–353, RSC Publishing, Cambridge, UK.

Zhou X, Zhuo X, Xie F, Kluetzman K, Shu YZ, Humphreys WG, and Ding X (2010) Role of CYP2A5 in the clearance of nicotine and cotinine: insights from studies on a *Cyp2a5*-null mouse model. *J Pharmacol Exp Ther* **332**:578–587.

Zhou X, Wei Y, Xie F, Laukaitis CM, Karn RC, Kluetzman K, Gu J, Zhang QY, Roberts DW, and Ding X (2011) A novel defensive mechanism against acetaminophen toxicity in the mouse lateral nasal gland: role of CYP2A5-mediated regulation of testosterone homeostasis and salivary androgen-binding protein expression. *Mol Pharmacol* **79**:710–723.

Zhou X, Zhang X, Weng Y, Fang C, Kaminsky L, and Ding X (2009) High abundance of testosterone and salivary androgen-binding protein in the lateral nasal gland of male mice. *J Steroid Biochem Mol Biol* **117**:81–86.

Zhou X, D'Agostino J, Xie F, and Ding X (2012a) Role of CYP2A5 in the bioactivation of the lung carcinogen 4-(methylnitrosamino)-1-(3-pyridyl)-1-butanone in mice. *J Pharmacol Exp Ther* **341**:233–241.

Zhou X, D'Agostino J, Li L, Moore CD, Yost GS, and Ding X (2012b) Respective roles of CYP2A5 and CYP2F2 in the bioactivation of 3-methylindole in mouse olfactory mucosa and lung: studies using *Cyp2a5*-null and *Cyp2f2*-null mouse models. *Drug Metab Dispos* **40**:642–647.

Zhuo X, Gu J, Behr MJ, Swiatek PJ, Cui H, Zhang QY, Xie Y, Collins DN, and Ding X (2004) Targeted disruption of the olfactory mucosa-specific *Cyp2g1* gene: impact on acetaminophen toxicity in the lateral nasal gland, and tissue-selective effects on Cyp2a5 expression. *J Pharmacol Exp Ther* **308**:719–728.

Address correspondence to: Dr. Xinxin Ding, Wadsworth Center, New York State Department of Health, Empire State Plaza, Box 509, Albany, NY 12201-0509. E-mail: xding@wadsworth.org